Journal of
Mechanics of
Materials and Structures

WRINKLED MEMBRANES
PART I: EXPERIMENTS

Y. Wesley Wong and Sergio Pellegrino

Volume 1, Nº 1 January 2006

mathematical sciences publishers

JOURNAL OF MECHANICS OF MATERIALS AND STRUCTURES
Vol. 1, No. 1, 2006

WRINKLED MEMBRANES PART I: EXPERIMENTS

Y. WESLEY WONG AND SERGIO PELLEGRINO

This paper presents a detailed experimental study of the evolution and shape of reversible corrugations, or *wrinkles*, in initially flat, linear-elastic and isotropic thin foils subject to in-plane loads. Two sets of experiments were carried out, on a rectangular membrane under simple shear and on a square membrane subjected to two pairs of equal and opposite diagonal forces at the corners. Salient findings are that: the wrinkle profile is generally well approximated by a half sine wave in the longitudinal direction, with constant or linearly-varying transverse wavelength; sudden changes in the shape of the membrane, accompanied by changes in the number of wrinkles, occur in both cases; in the sheared membrane the wrinkle pattern remains essentially unchanged for increasing shear displacement, whereas in the square membrane a large diagonal wrinkle appears when the corner load ratio is around 3.

1. Introduction

Thin, prestressed membranes are a key element of the next generation of spacecraft, to provide deployable mirror surfaces, solar collectors, sunshields, solar sails, etc. While some of these applications demand very smooth surfaces, and hence membranes that are biaxially prestressed, for several other applications slightly nonsmooth membranes are acceptable, provided that the size and shape of the deviation from the nominal shape are sufficiently small. The realization of wrinkled or partially wrinkled membrane structures, as opposed to structures with totally smooth surfaces is often much simpler and cheaper [Jenkins 2001], and therefore, for those applications in which a slightly wavy surface may be acceptable, engineers are now faced with the task of estimating the extent and amount of waviness.

This paper, the first in a series of three, aims to observe the formation, evolution, and shape of reversible corrugations, or *wrinkles* that form in initially flat, linear-elastic and isotropic thin foils, or *membranes*, under the action of in-plane loads. Initial imperfections, arising say from the presence of permanent creases due to previous folding of the membrane, are not considered. The experimental observations made in the present paper form the basis for an analytical model that will explain

Keywords: plate buckling, membrane structures, wrinkling.

and identify the key characteristics of wrinkles and provide simple predictions for the wavelength and amplitude of the wrinkles; see [Wong and Pellegrino 2006a]. Detailed numerical simulations will appear in [Wong and Pellegrino 2006b].

Previous work on wrinkled membranes has focussed mainly on the load transfer characteristics of wrinkled membranes and the associated, nonlinear constitutive relationships. Wrinkled shear webs were first investigated by Wagner [1929] and later by Reissner [1938] and Mansfield [Mansfield 1968; 1989], and these studies established wrinkled membranes as a very useful and efficient structural element for lightweight structures. Stein and Hedgepeth [1961], followed by many others, investigated the nonlinear load-displacement or moment-rotation relationship of partially wrinkled membrane structures.

Only recently have the wrinkle details, such as wrinkle pattern, wavelength and amplitude, been of interest to researchers [Cerda et al. 2002; Wong and Pellegrino 2002; Epstein 2003], so it is appropriate to begin with an experimental characterization of the way in which wrinkles form and develop in simple, thin membrane structures. Particular aims of the present study will be to examine how wrinkles change in response to the applied loads and also how repeatable any particular pattern of wrinkles is when the loads are removed and then reapplied, in order to establish particular features of their behaviour that one needs to be aware of when setting out to develop appropriate analytical or computational models.

Hence, this paper will present experiments that were carried out first on a rectangular membrane whose long edges are sheared uniformly, thus forming a series of approximately uniform diagonal wrinkles, and secondly on a square membrane subjected to two pairs of equal and opposite diagonal forces at the corners, where the ratio between the magnitude of the forces had different values. In each experiment the wrinkle pattern was carefully measured, and the wrinkle wavelength and amplitude were obtained from the measurements.

The layout of the paper is as follows. Section 2 presents a brief review of previous experimental work on wrinkled membranes. Section 3 describes the apparatus for the two sets of experiments. Sections 4 and 5 present the experimental results obtained from the membrane in shear and from the square membrane, respectively. Section 6 concludes the paper.

2. Review of previous work

Early experiments on wrinkled membranes mainly focussed on the measurement of overall response parameters, such as the end rotation of a pressurized cylinder in pure bending [Stein and Hedgepeth 1961] or the torque-rotation relationship of a stretched circular membrane attached to a central hub [Stein and Hedgepeth 1961; Mikulas 1964]. These particular experimental studies were carried out to validate

wrinkling theories developed specifically to analyse partially wrinkled membranes. They also intended to confirm that the membrane retained most of its stiffness after wrinkling had first occurred, although a notable softening was in fact observed with the growth in the extent of the wrinkled regions.

In another classical study, Mansfield [1968; 1970] determined the orientation of the wrinkle lines in membranes with different shapes, for different boundary conditions. Only qualitative correlations between theory and the experimental observations were attempted.

Performing detailed measurements on thin membranes is not easy, mainly because high accuracy noncontact measurement apparatus is needed. A set of carefully planned experiments, including accurate measurements of wrinkle details by using a capacitance proximity sensor, were carried out by Jenkins et al. [1998] on a square Mylar membrane subjected to different combinations of shear and tension forces. These experiments showed that both the wrinkle amplitude and the number of wrinkles increase with the applied shear force, but decrease with the tension force. The reverse relationship was found between the wrinkle wavelength and the applied forces.

The same measurement technique was later extended by Blandino et al. [2001] to measure the surface profile of a thin, aluminized 0.5 m square Kapton® membrane subjected to four corner forces, to include the effects of thermal gradients within the membrane. Blandino et al. [2001] also produced a complete out-of-plane displacement contour plot for the membrane using photogrammetry, and compared the two sets of measurements in the region near a corner of the membrane. Good agreement was observed, with an accuracy of up to ± 0.02 mm on the wrinkle amplitudes.

The main disadvantage of capacitance sensors is that they need a metallic surface target and the sensor must be in electrical contact with the membrane. As for photogrammetry, a large number of target points is required in order to capture fine wrinkle details and the postprocessing of the images can be time-consuming [Blandino et al. 2002a]. However, the latest applications of this technique, based on the commercial software package Photomodeler 4.0 [Blandino et al. 2003], have shown that this technique is making very rapid advances.

All of the work mentioned above was carried out on initially flat films. The effect of preexisting creases on the constitutive behaviour of thin foils has been investigated by Murphey [2000] and Papa and Pellegrino [2005].

3. Experimental techniques

In the present study we are interested in measuring the out-of-plane displacement/amplitude of wrinkles formed in a nominally flat membrane. The particular membrane that was used is a polyimide film made by DuPont, known as Kapton HN®. This film is already widely used for various spacecraft applications, because of its optical properties (e.g. excellent adhesion to metal films), electrical and thermal conductivity, and environmental compatibility and survivability. Some of these foils were supplied with a mirror surface finish, which made the selection of a suitable measurement device particularly challenging.

A Charge Coupled Device (CCD) laser displacement sensor, model LK-081 supplied by Keyence, was used for all experiments presented in this paper. Unlike conventional laser sensors, which use the whole light distribution in the beam spot and hence tend to be affected by the surface finish of the target surface, this particular device detects the pixel with the peak light intensity and uses triangulation to measure the distance from the laser to the reflecting surface. The device is positioned at a reference distance of 80 mm from the surface and has a measurement range of ± 15 mm, corresponding to a full output of ± 5 V (amounting to 3 mm/V), with a resolution of 3 μm.

The voltage output from the laser was logged to a Schlumberger SI 3531P data acquisition system set at 2 readings per second, and the position of the laser corresponding to each measurement was worked out by assuming that the laser travels at a uniform speed.

3.1. ***Laser scanning frame.*** The laser was mounted on a supporting unit attached via two linear guides to an Al-alloy frame; see Figure 1(a). The position of the supporting unit is controlled by a 10 mm diameter brass threaded rod, held by two end bearings and driven by a geared DC motor, whose speed is such that the laser is moved at a rate of 0.5 mm/s. The connection is through a floating nut, to avoid jamming. Although a small vibration is induced in the frame by the movement of the laser, it was found that the noise on the laser output was negligible.

The maximum travel of the laser, in the x-direction, defined in Figure 1(b), is approximately 400 mm.

3.2. ***Shear test apparatus.*** An apparatus to subject rectangular membranes to a state of simple shear was designed and constructed, in order to measure the profile of different sections of the membrane by means of the laser scanning frame described in Section 3.1.

This shear rig comprises a stiff base plate and two parallel blocks holding the longer edges of the membrane. One block is fixed and the other, which holds the

upper edge of the membrane, can be moved along the x-axis, in either sense, to apply shear displacements. Movement in the y-direction is not allowed.

Four linear bearings support the movable edge of the membrane, whose position can be precision controlled by means of a threaded rod, and monitored with a digital displacement gauge with an accuracy of ± 0.05 mm.

First, the membrane is attached to the moving edge. Then, before clamping the fixed edge, a small initial stress is applied in the y-direction by means of a system of counterweights, connected to the membrane by Kapton® tabs through Kevlar® cords running over closely spaced pulleys. The surplus membrane, cords, counterweights, etc. are removed after tightening the fixed edge clamping strip. The complete experiment set-up is shown in Figure 1(b).

The overall dimensions of the base plate are 430 mm $\times$ 440 mm. The whole rig was constructed of steel and its parts were sized on the basis that the maximum deflection should be less than 0.1 mm under a maximum load of 1.7 N/mm from the membrane (corresponding to the ultimate stress of Kapton HN®, which is 69 N/mm^2, and considering 0.025 mm thick membranes [DuPont 2001]). The maximum normal stress in any test described in this paper will be less than half this ultimate value, to stay well within the linear range of the material. Wong [2003] has measured an average Young's Modulus of 3500 N/mm^2 and an average Poisson's ratio of 0.31 in Kapton HN®, over a range of three film thicknesses (0.0125, 0.025, and 0.05 mm) and for strains up to 0.8%.

3.3. ***Square membrane apparatus.*** A 650 mm square frame was designed to hold a 500 mm square membrane and apply point loads at the four corners. This frame was built by welding four 25 mm $\times$ 1.5 mm steel square hollow sections, with a diagonal bracing member welded at the back. Four 12 mm square bars were welded across the four corners of the frame. These provide end attachments for the membrane, through 4 mm holes drilled through each bar.

Corner attachments, able to withstand a maximum tension of 20 N without inducing any plastic deformation of the membrane, were made as follows. The corners of the membranes were cut at 45° to the sides, to a width of 25 mm; 1.5 mm diameter steel pins were attached to the cut edges, with a 25 mm wide by 40 mm long strip of Kapton® adhesive tape doubled back over the membrane (thus, each pin forms a 25 mm wide spreader bar, which distributes the applied load as surface tractions on either sides of the membrane, over a patch of 25 mm $\times$ 20 mm); a 0.9 mm diameter Kevlar® cord was used to connect the centre of the pin to a strain gauged turn-buckle. The connection between the turn-buckle and the cord was designed such that minimum distortions were introduced during tensioning and the cord length could be adjusted at any stage of the experiment.

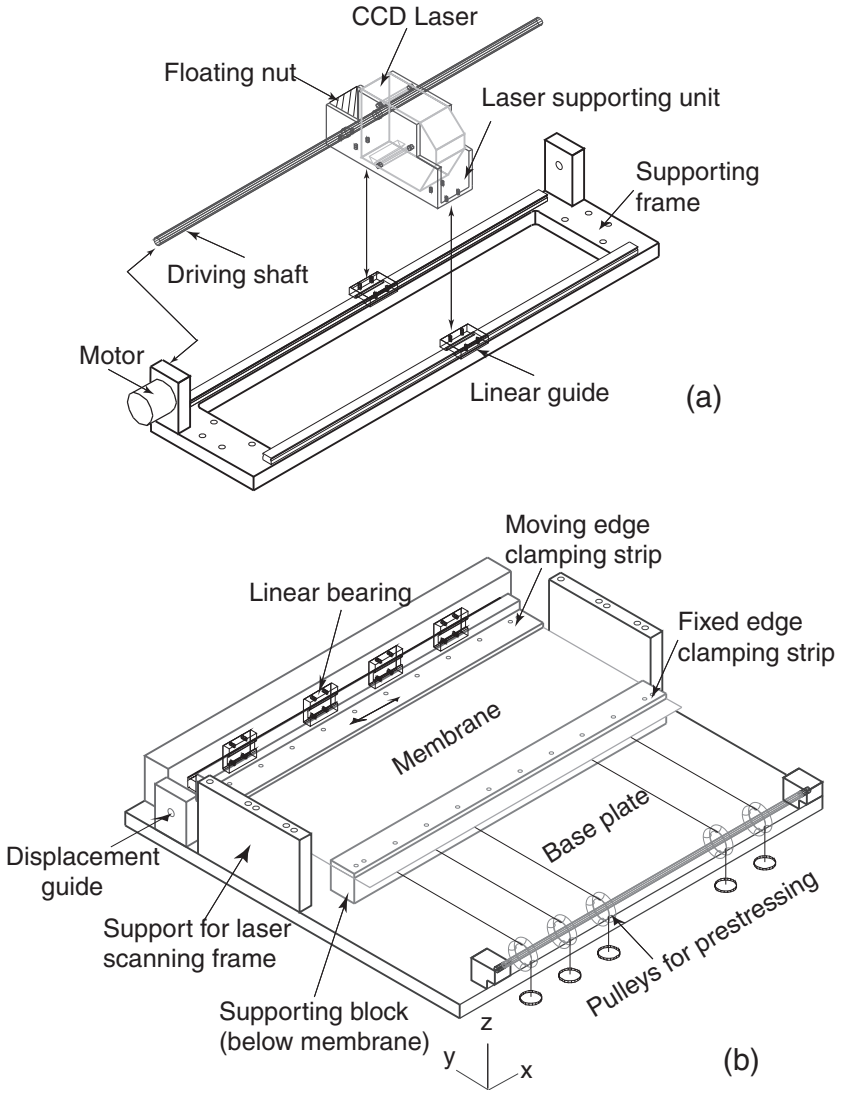

Figure 1. (a) Laser scanning frame, (b) Shear-rig.

The same type of connection was used for all four corners of the membrane. Thus, the tension force applied at each corner could be varied to produce different load ratios, T_1/T_2. Note that, for equilibrium, only two forces can be varied independently. Hence, two strain meters were used to monitor the load levels.

The load frame was designed such that the effect of gravity on the wrinkles formed in the membrane could be compared, for any chosen load condition, by holding the membrane either vertical or horizontal.

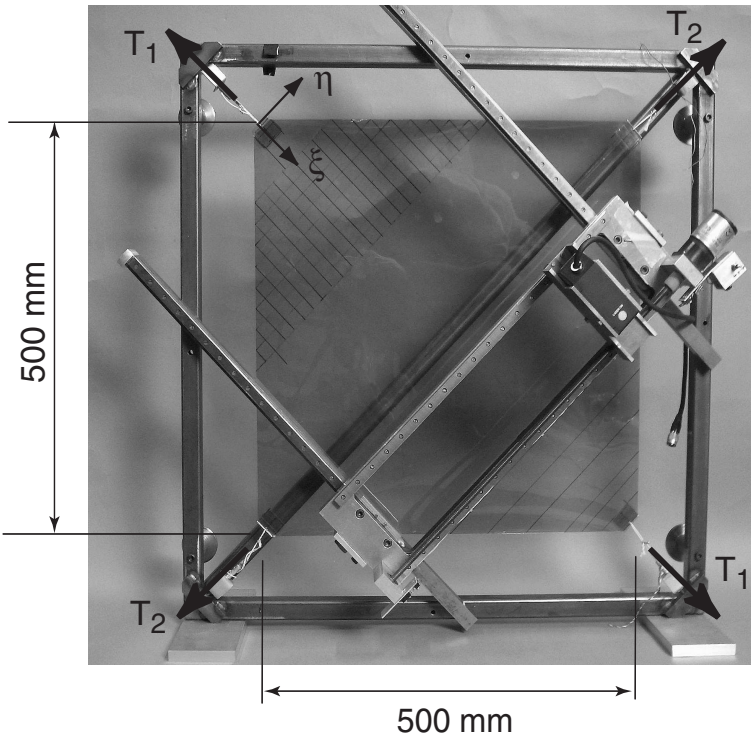

Figure 2. Square frame experimental set-up, in vertical configuration.

The laser scanning frame described in Section 3.1 was attached to the square frame through linear bearings running on guide rails at 45° to the sides of the frame. The complete experimental set-up is shown in Figure 2. (An additional local coordinate system, ξ, η, is defined in this figure.) The use of the linear guides enables the laser to scan, in the η direction, profiles of the membrane with different values of ξ. Two pairs of corner tension forces, T_1 and T_2, are also indicated in the figure.

4. Membrane in shear

The main purpose of subjecting rectangular membranes to simple shear was to investigate the variation of the wrinkle parameters — that is, the relationship between out-of-plane displacement and wavelength — with the magnitude of the applied shear displacement. The boundary conditions are relatively simple in this case; the two long edges of the membrane are held at a fixed distance while the two side edges are unrestrained, and so the wrinkles arrange themselves to form a repeating pattern. All test results presented in this section were obtained on 380 mm wide membranes with a height, between the supports, of 128 mm.

4.1. ***Wrinkle pattern.*** The overall wrinkle pattern (see Figure 3) shows that, apart from two "fan" regions near the short edges of the membrane, the wrinkles are inclined at an angle of 45° to the upper and bottom edges of the shear-rig. They are also parallel to each other, of course.

As the shear displacement was gradually increased, the wrinkle pattern remained essentially unchanged, all the wrinkles in the middle being inclined at approximately 45° to the edges, as before, and the two side fans becoming more distorted. The size of the central wrinkled region, bounded by the two fan regions, remained almost unchanged, although the number of wrinkles increased when the shear displacement was increased. Figure 3 shows the wrinkle patterns corresponding to shear displacements of 0.5 mm, 1.0 mm, 2.0 mm and 3.0 mm (for which the maximum normal strain is 1.2%, and so Kapton® begins to behave nonlinearly), for a 0.025 mm thick film.

Repeating this test on foils of different thickness showed that *the number of wrinkles decreases when the thickness of the membrane is increased*, the shear displacement being equal. An extensive set of photographs of these wrinkle patterns can be found in Wong [2003].

4.2. ***Wrinkle profile.*** The wrinkle details were further investigated by scanning the membranes across the middle (section A-A in Figure 3) with the CCD laser.

The laser measurements provide the out-of-plane displacement of the membrane, w. Plotting this height vs. the position of the laser is a useful tool for studying the characteristics of the wrinkles. Figure 4 shows four plots of this kind, based on measurements taken half-way between the two long edges of the membrane ($y =$ 64 mm) on a 0.025 mm thick Kapton® film. The four plots, for shear displacements of $\delta = 0.5$ mm, $\delta = 1.0$ mm, $\delta = 2.0$ mm, and $\delta = 3.0$ mm, which correspond one by one to the wrinkle patterns shown in Figure 3.

A common feature of the plots shown in Figure 4, see for example Figure 4(b), is the presence of three distinct regions, as follows. Regions (i) and (iii) consist of two high peaks each, close to the free edges on the sides of the membrane. Region (ii), in the middle, is characterised by fairly uniform wrinkles and it will be shown in Part 2 of this paper series that the key characteristics of the wrinkles in Region (ii) can be captured with a simple analytical model.

In Figure 4 it can be noticed that the number of wrinkles increases with the applied shear displacement. More precisely, if each crest in these plots is counted as a wrinkle, the plots show that there are 15 wrinkles for $\delta = 0.5$ mm, 17 for $\delta =$ 1.0 mm, 18 for $\delta = 2.0$ mm, and 19 for $\delta = 3.0$ mm. Also, it was observed during the experiments that when δ was increased gradually and monotonically, changes in the numbers of wrinkles occur *suddenly*. A detailed numerical simulation, described in the third paper in this series [Wong and Pellegrino 2006b], shows that any change

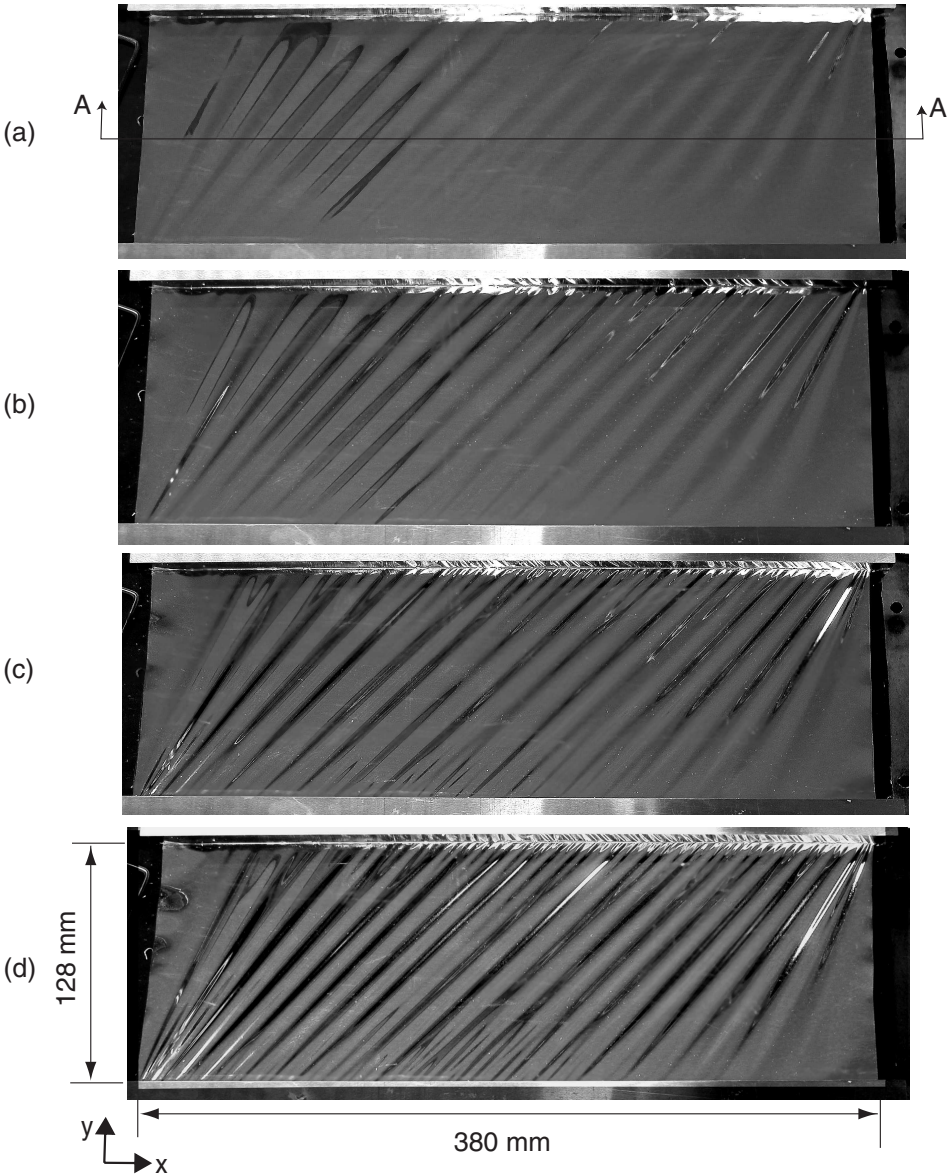

Figure 3. Wrinkle patterns for a 0.025 mm thick Kapton® film under shear displacements of (a) $\delta = 0.5$ mm, (b) $\delta = 1.0$ mm, (c) $\delta = 2.0$ mm, and (d) $\delta = 3.0$ mm.

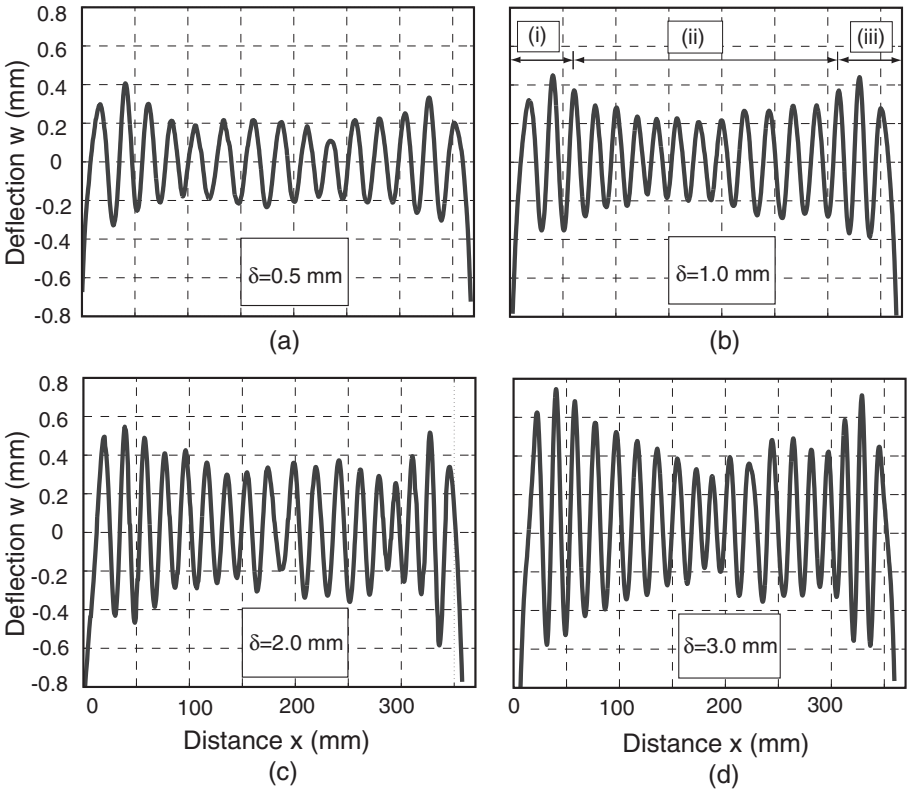

Figure 4. Section A-A of 0.025 mm thick Kapton® film for shear displacements of (a) $\delta = 0.5$ mm, (b) $\delta = 1.0$ mm, (c) $\delta = 2.0$ mm, and (d) $\delta = 3.0$ mm.

in the number of wrinkles is the effect of an instability (mode jumping) that usually occurs near the edge of the membrane.

Another important observation that can be made from Figure 4 is that both the wrinkle amplitudes and the number of wrinkles increase, whereas their corresponding wavelengths decrease when δ is increased.

Figure 5 shows the evolution in the profile of the membrane during an unload–reload cycle, beginning immediately after the load cycle depicted in Figure 4. It is interesting to compare the membrane profiles that correspond to the same value of the shear displacement, but at different stages of the loading cycle. For example, for $\delta = 2.0$ mm the number of wrinkles is 18 when δ is increasing — see Figure 4(c) — but it is 19 when δ is decreasing — see Figure 5(b). Similarly, for $\delta = 0.5$ mm their numbers are 15 and 19, respectively.

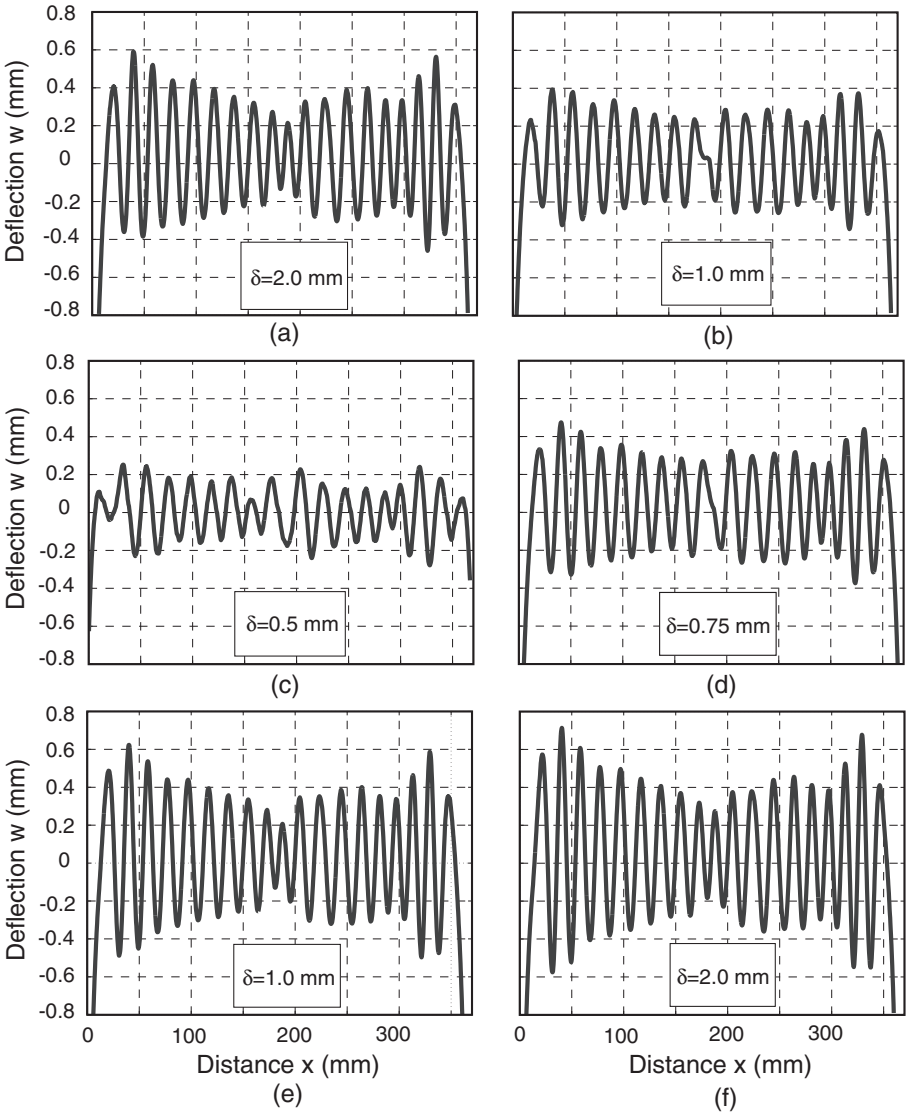

Figure 5. Section A-A of 0.025 mm thick Kapton® film under shear, during (a–c) unloading and (d–f) reloading.

After the first unloading small residual imperfections were noted, resulting from slippage/yielding of the material near the clamped edges. Upon reloading, these imperfections have the effect of driving the membrane more rapidly towards its final configuration (with 19 wrinkles) much earlier, compared to the nearly perfect membrane used in the first loading cycle.

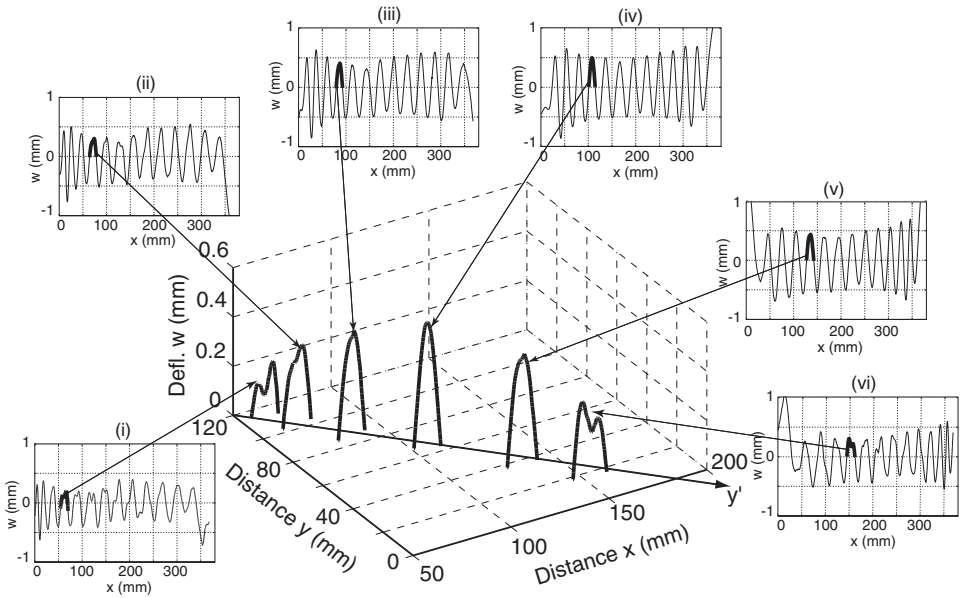

Figure 6. Three-dimensional view of half-wrinkle in sheared membrane.

4.3. ***Wrinkle shape.*** The maximum wrinkle amplitude can be expected to occur half-way between the two clamped edges of the membrane. In order to verify this, and to measure the longitudinal shape of a wrinkle, additional profiles of the membrane were measured at the following distances from the fixed edge, $y = 15$ mm, $y = 30$ mm, $y = 64$ mm, $y = 85$ mm, $y = 105$ mm and $y = 110$ mm, for the same shear displacement. These profiles, labelled (i) to (vi), are shown in Figure 6. The central part of this figure shows a three-dimensional reconstruction of the shape of a particular half-wrinkle, based on corresponding segments of the six profiles. Then, having defined a new axis y' at 45° to x and y, as shown in Figure 6, the amplitudes of the six selected crests have been plotted in Figure 7 together with a half sine wave whose amplitude has been scaled to match the wrinkle amplitude at point (iv). The shape of the wrinkle can be described quite accurately by this simple mode-shape.

In addition to obtaining information on the amplitude of a wrinkle, the half-wavelength of this particular wrinkle — given by the base width of the six crests in Figure 6 — can be seen to remain approximately constant, except when it approaches the end supports; see Figure 6(i) and (vi). This particular effect may be due to localised deformation imposed by the clamping strips; additional small wrinkles appear in these end regions. Also note that large displacements occur at the free side edges.

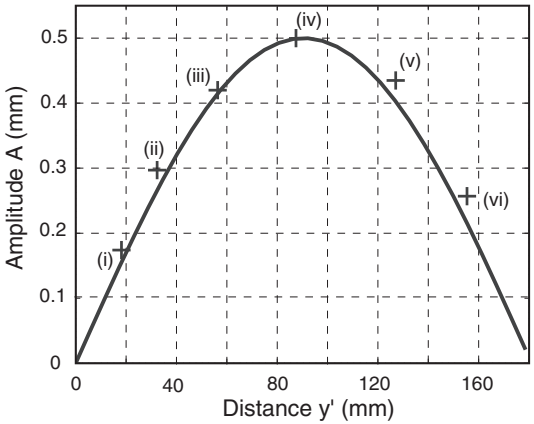

Figure 7. Comparison of longitudinal wrinkle profile with a sinusoidal mode shape, for sheared membrane.

4.4. ***Discussion.*** This study has revealed a number of important characteristics of wrinkles in thin rectangular membranes under simple shear.

It was already observed in [Mansfield 1989], and it has been confirmed, that the wrinkle pattern comprises a general "parallelogram" of wrinkles in the central region, containing approximately uniform wrinkles at 45°, plus two triangular fan regions which include a small highly stressed corner region and a triangular slack region, near the side edges. The extent of these fan regions remains approximately unchanged when the magnitude of the shear displacement δ is varied.

It has been established that in the uniformly wrinkled region the wrinkle amplitude and wavelength vary with δ. More precisely, the wrinkle wavelength decreased with increasing δ, although the rate of change was found to decrease as δ grew larger. Conversely, both the amplitude and the number of the wrinkles were found to initially increase with δ. For $\delta > 1.5$ mm (corresponding to a normal strain of 0.6% along the wrinkles) the wrinkle pattern was found to have become stable: only one more wrinkle could be formed, and only by increasing δ to almost 3 mm.

The average wrinkle wavelength and average amplitude (taken as the average wrinkle height in the central region, discarding the higher peaks at the corners) for Kapton® membranes of three different thicknesses have been plotted against the shear displacement in Figure 8.

5. Membrane under corner loads

In the case of the square membrane subject to corner loads, two load cases were investigated. First, the membrane was subjected to a series of gradually increasing symmetrical tension loads $T\,(= T_1 = T_2)$ at its four corners. Second, one pair of

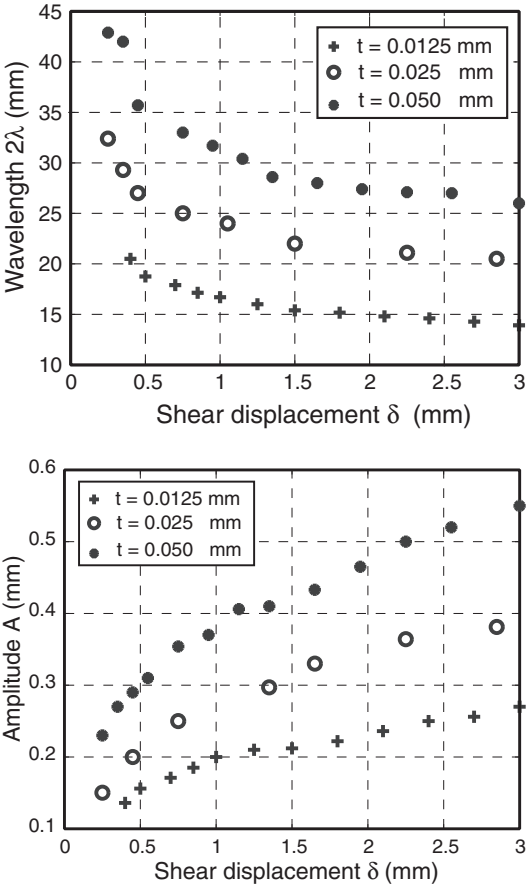

Figure 8. Average wrinkle wavelengths measured in the x-direction (top) and average wrinkle amplitudes (bottom) in sheared membranes of different thicknesses.

loads, T_2, was kept constant while the other pair, T_1, was increased, to study the effects of different load ratios. The associated wrinkle details were measured for every load case and for different membrane thicknesses. Here we present results from a set of experiments on a 0.025 mm thick, 500 mm by 500 mm Kapton® membrane.

5.1. ***Symmetric loading ($T_1 = T_2$).*** The membrane was first loaded up to 5 N at all four corners and the wrinkle profile was scanned with the CCD laser at six different locations, corresponding to the following values of the coordinate ξ (measured from a corner of the membrane loaded by one of the forces T_1): $\xi = 35$ mm, $\xi = 53$ mm, $\xi = 70$ mm, $\xi = 105$ mm, $\xi = 141$ mm, and $\xi = 177$ mm. (The

coordinate system ξ, η is defined in Figure 2.) After all six profiles had been scanned, one pair of loads, T_1, was increased to 10 N and finally to 20 N, and all scans were repeated.

Wrinkle profiles were produced by plotting the membrane out-of-plane displacement, w, against the distance η across the membrane (measured from the edge of the membrane) for two load levels, $T = T_1 = T_2 = 5$ N and $T = T_1 = T_2 = 20$ N. The results are presented in Figure 9. Note that the membrane slopes down from left to right, by about 0.5 mm, and this effect needs to be discounted when measuring the wrinkle amplitudes. Blandino et al. [2002a] carried out an almost identical experiment, but using triangular tabs at the corners of the membrane.

Examining the plots in Figure 9 shows that for increasing distance from the corner of the membrane, first the amplitude of the wrinkles increases, reaching a maximum at $\xi \approx 105$ mm, and then starts decreasing. The wrinkles become vanishingly small when $\xi \approx 180$ mm; the central part of the membrane is unwrinkled. Also note that, if edge effects are neglected, the wrinkle amplitudes for symmetrical loading are quite small, and indeed much smaller than will be observed under asymmetric loading, in the next section.

An interesting observation is that the extent of the wrinkled regions in the membrane remains essentially the same, despite a four-fold increase in the load level, and wrinkle amplitude and wavelength are reasonably uniform, apart from the edges of the membrane. However, the number of wrinkles increased when the load was increased, as already observed by Blandino et al. [2002b], and did so suddenly, thus showing mode-jumping as already observed in the shear experiment presented in Section 4.2. Figure 9(d) shows that the number of wrinkles increased from four when $T = 5$ N, to five when $T = 20$ N. The wrinkle wavelength decreases correspondingly, and the wrinkle amplitude is also observed to have decreased with the higher loads.

Figure 9 also shows that the wrinkle profiles at the smaller load, $T = 5$ N, are less uniform than at the higher load, $T = 20$ N. Therefore, rather than considering individual wrinkles, average values will be used to study general trends.

A photograph showing the overall wrinkle pattern for $T = T_1 = T_2 = 5$ N is shown in Figure 10(a). It can be seen that there are four, symmetric wrinkled regions, radiating from each corner, plus a large central region which is visibly free of wrinkles. These visual observations agree with the earlier discussion of the wrinkle profiles.

5.2. ***Asymmetric loading.*** Under symmetric loading the wrinkle amplitudes had been found to be small. In the second load case, a diagonal wrinkle with larger features was formed by increasing the load ratio, T_1/T_2. T_2 was kept fixed at 5 N, and T_1 was gradually increased from 5 N to 20 N.

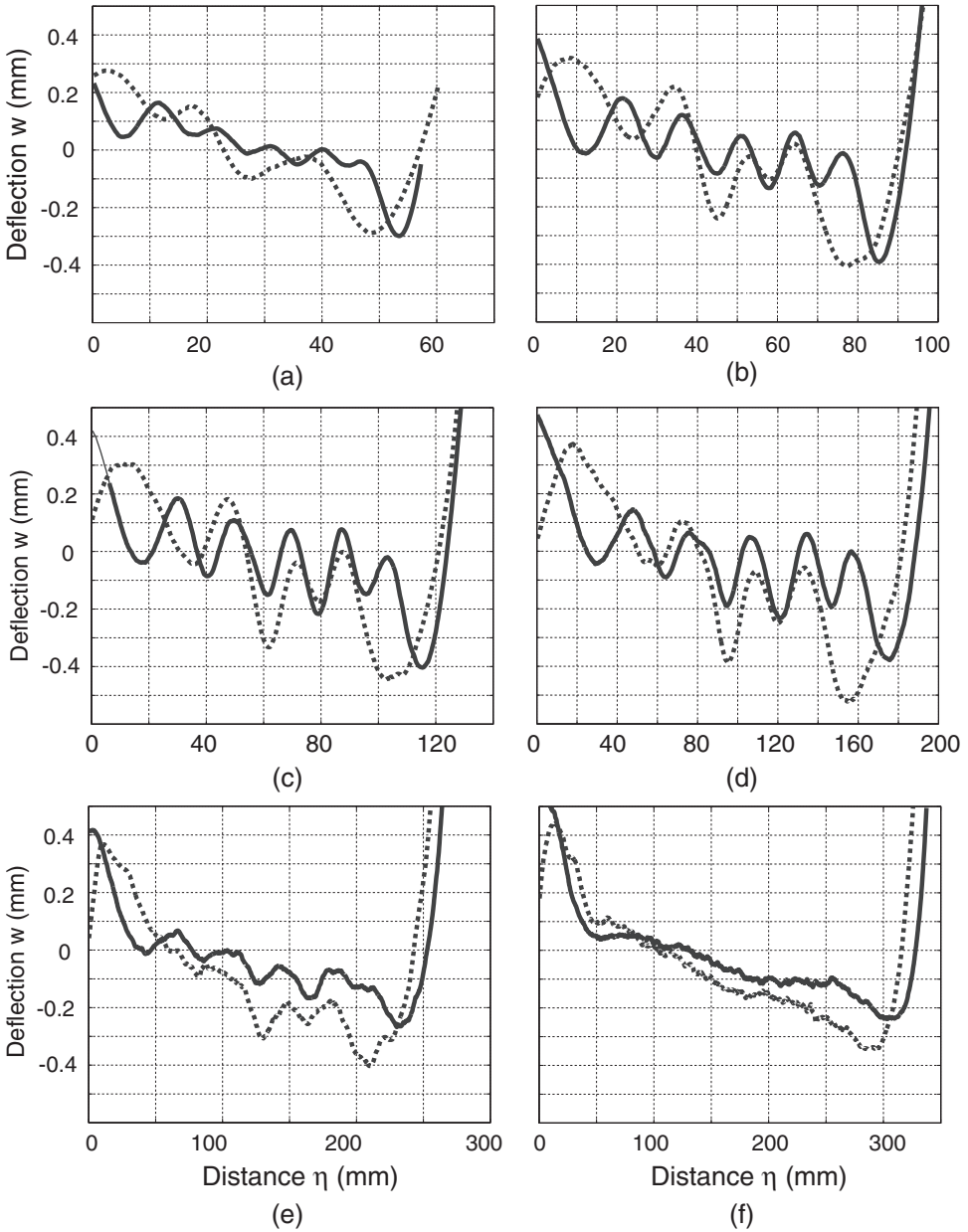

Figure 9. Wrinkle profiles in 0.025 mm thick, square Kapton® membrane, for $T = T_1 = T_2 = 5$ N (dashed) and $T = T_1 = T_2 = 20$ N (solid), at following distances from corner (a) $\xi = 35$ mm, (b) $\xi = 53$ mm, (c) $\xi = 70$ mm, (d) $\xi = 105$ mm, (e) $\xi = 141$ mm and (f) $\xi = 177$ mm.

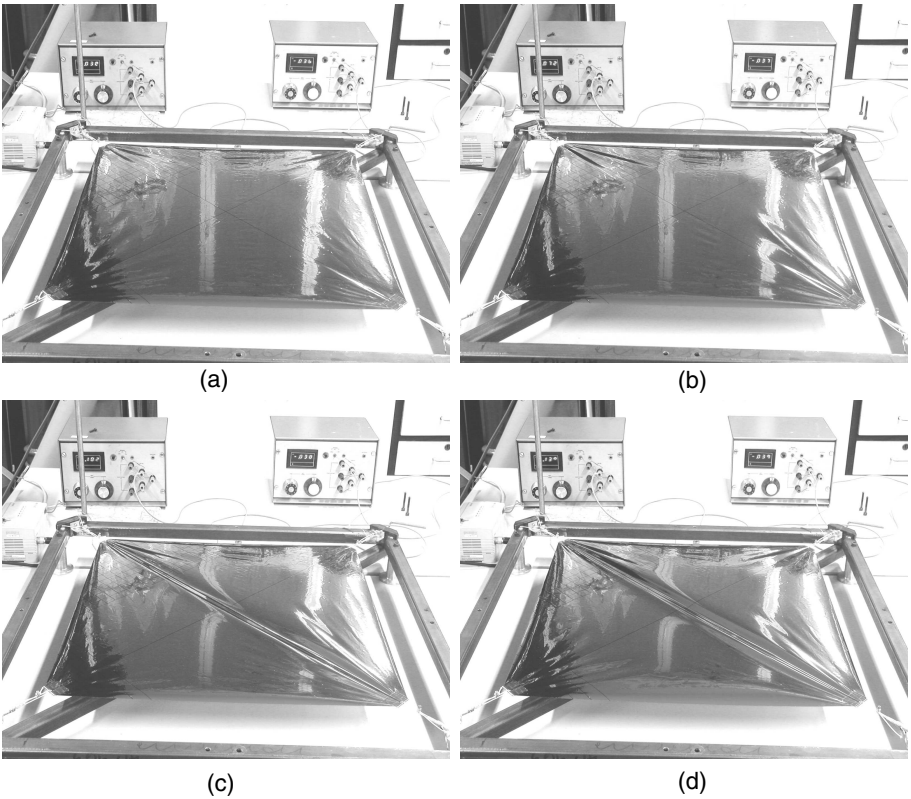

Figure 10. Wrinkle pattern in 0.025 mm thick square Kapton® membrane for (a) $T_1/T_2 = 1$, (b) $T_1/T_2 = 2$, (c) $T_1/T_2 = 3$ and (d) $T_1/T_2 = 4$.

Figure 10 shows the overall wrinkle pattern in the membrane, for different load ratios. The wrinkle pattern was generally unchanged for T_1/T_2 up to 2, again with wrinkles radiating from the corners and the central wrinkle-free region gradually becoming smaller as the load ratio increased. The appearance of the membrane changed when T_1/T_2 was increased from 2 to 3; a diagonal wrinkle formed between the more heavily loaded corners and this diagonal wrinkle became more dominant, with a larger amplitude and wavelength when the maximum load ratio of $T_1/T_2 = 4$ was applied, as shown in Figure 10(d).

To monitor the growth of this diagonal wrinkle the profile of the membrane was measured at three cross-sections, $\xi = 105$ mm, $\xi = 177$ mm and $\xi = 355$ mm, for each load ratio. These profiles are plotted in Figure 11.

The most noticeable feature in these figures is a very large central wrinkle at $T_1/T_2 = 4$, with correspondingly large edge displacements, but not in Figure 11(c)

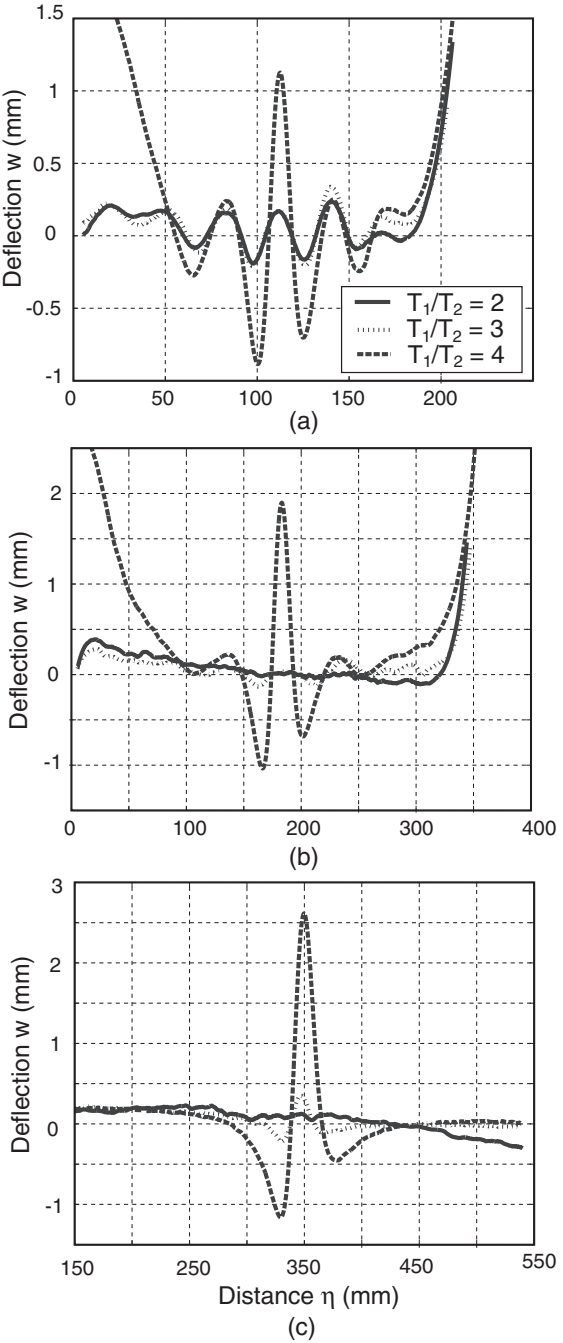

Figure 11. Wrinkle profiles for 0.025 mm thick, square Kapton® membrane at (a) $\xi = 105$, (b) $\xi = 177$ and (c) $\xi = 355$ mm for different load ratios.

which corresponds to a section of the membrane containing the other two corners of the membrane. The figure also shows that there are still no wrinkles beyond $\xi = 177$ mm for $T_1/T_2 = 2$. But at $T_1/T_2 = 3$, a wrinkle has started to form across the centre of the membrane, at $\xi = 355$ mm.

Similar experiments were conducted on two more Kapton® films, one thinner (0.0125 mm thick) and one thicker (0.05 mm). Both films exhibited the same behaviour as that described above for the 0.025 mm thick film. Photographs showing the wrinkle patterns observed in these films, under different load ratios can be found in [Wong 2003].

The situation can be summarised as follows. For load ratios up to 2, only corner wrinkles form in any of these membranes. These wrinkles are more obviously visible in the thinnest film, where many more wrinkles were observed, and are hardly noticeable in the thickest film. At $T_1/T_2 = 3$ a diagonal wrinkle was noticed in the central region of all films, and this wrinkle dominates the wrinkle pattern at the maximum load ratio of 4. In all cases, there were two small wrinkled regions in the other two corners of the membrane. The magnitudes of these smaller wrinkles were not measured.

5.3. ***Discussion.*** Average wrinkle wavelengths and amplitudes were obtained from the plots in Figure 9, and also from analogous plots for membranes of two other thicknesses; they are shown in Figure 12. These average values were computed over the central portion of the membranes, where "more uniform" wrinkle profiles are observed, and thus disregarding the side edges. Because the wrinkle profiles at lower stress levels had been found to be less uniform, the average wavelengths and amplitudes were computed from the wrinkle profiles measured at the highest load levels, which were $T = 10$ N for the 0.0125 mm thick film and $T = 20$ N for the 0.025 mm and 0.05 mm thick films.

The wrinkle wavelengths for all three membranes were found to increase approximately linearly with the distance from the corner, see Figure 12. This observation is consistent with the radial wrinkle pattern pointed out in Figure 10.

Figure 13 shows the longitudinal profile of an average wrinkle, obtained by plotting the average wrinkle amplitudes versus distance from the corner of the membrane. For the two thinner films these amplitudes first increase and then decrease, after attaining a maximum value approximately in the middle of the wrinkle profile, and generally both the wavelength and amplitude increase with the thickness of the membrane.

However, the thickest membrane did not follow these trends; it attained its maximum wrinkle amplitude much closer to the corner, at $\xi = 70$ mm. This difference is probably because the load-to-thickness ratio, which was kept constant in the 0.0125 mm and 0.025 mm thick membranes, was halved in the 0.05 mm thick

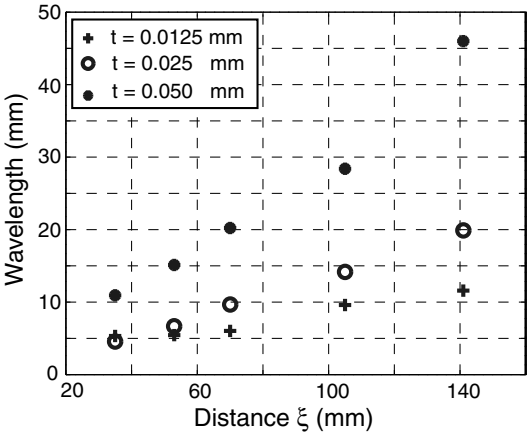

Figure 12. Average wrinkle wavelength in corner region of square membrane, vs. distance from corner, for $T_1/T_2 = 1$.

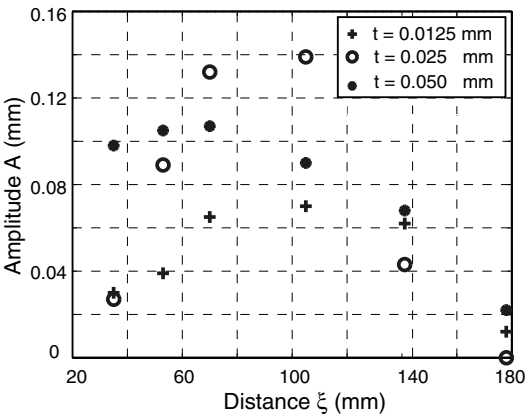

Figure 13. Longitudinal profile of corner wrinkles in square membrane, for $T_1/T_2 = 1$.

membrane, because the corner attachments could only carry a maximum load of only 20 N.

Thus, the profiles of the wrinkles in the thinner membranes can, again, be described quite accurately by a half sine wave, but this approximation becomes less accurate for thicker membranes under low stress.

For the asymmetric load case, the cross-sectional plots shown in Figure 11 have provided insight into the interaction between the large diagonal wrinkle and the (much smaller) corner wrinkles. Several other interesting details can be noted in

these plots. For example, the wrinkle profile can be seen to have become (almost) anti-symmetric about a central diagonal line. Also, at the highest load ratio, $T_1/T_2 = 4$, both the width and the amplitude of the central diagonal wrinkle were found to increase with the distance from the corner. A detailed study by Wong [2003] has confirmed that for all three membrane thicknesses both of these parameters reach their maximum magnitude at the centre of the membrane, at $\xi = 355$ mm. The wrinkle profiles beyond this point are the mirror image of the profile in the first half membrane.

6. Conclusion

In addition to the points made in the detailed discussion presented at the end of each experiment, in Sections 4.4 and 5.3, there are some general features of the problems studied that should also be noted.

First, the two experiments presented in this paper share a number of common features, as follows.

- Wrinkle profile; well approximated by a half sine wave in the longitudinal direction with linearly-varying transverse wavelength in the transverse direction. Indeed, there is no wavelength variation at all in the sheared membrane problem.
- Mode jumping, that is, a sudden change in the number of wrinkles, occurs both in the central, uniformly wrinkled, part of the sheared membrane and in the corner regions of the square membrane. In both cases, this is due to the fact that only an integral number of wrinkles is allowed by the boundaries.

Second, on the other hand, some important differences have become apparent, as follows.

- Wrinkle pattern: its evolution is different in the two cases. Whereas in the sheared membrane the wrinkle pattern remains essentially unchanged for increasing shear displacement, in the square membrane a large diagonal wrinkle appears when the corner load ratio is around 3.
- Average stress: due to the presence of stress concentrations at the corners of the tabs, wrinkles appear in this membrane even though the average stress is rather low. One effect is that the wrinkle characteristics in the square membrane experiments appear to be more repeatable than in the sheared membrane, where slippage/yielding is prone to occur along the edges.

Although none of the features noted is particularly surprising, these are useful points to come back to in the following two papers in this series.

Acknowledgements

The authors thank Professor C. R. Calladine, FRS, for useful discussions and suggestions. Helpful suggestions by an anonymous reviewer are acknowledged. Financial support from NASA Langley Research Center (research grant NAG-1-02009, technical monitor Dr. K. Belvin) and the Cambridge Commonwealth Trust is gratefully acknowledged.

References

[Blandino et al. 2001] J. R. Blandino, J. D. Johnston, J. J. Miles, and J. S. Soplop, "Thin film membrane wrinkling due to mechanical and thermal loads", in *42th AIAA/ASME/ASCE/AHS/ASC Structures, Structural Dynamics and Material Conference and Exhibit*, 2001. AIAA-2001-1345.

[Blandino et al. 2002a] J. R. Blandino, J. D. Johnston, and U. K. Dharamsi, "Corner wrinkling of a square membrane due to symmetric mechanical loads", *J. Spacecraft Rockets* **39** (2002), 717–724.

[Blandino et al. 2002b] J. R. Blandino, J. D. Johnston, J. J. Miles, and U. K. Dharamsi, "The effect of asymmetric mechanical and thermal loading on membrane wrinkling", in *43rd AIAA/ASME/ASCE/AHS/ASC Structures, Structural Dynamics and Material Conference and Exhibit*, 2002. AIAA-2002-1369.

[Blandino et al. 2003] J. R. Blandino, R. Pappa, and J. Black, "Model identification of membrane structures with videogrammetry and laser vibrometry", in *44th AIAA/ASME/ASCE/AHS/ASC Structures, Structural Dynamics, and Material Conference and Exhibit*, 2003. AIAA-2003-1745.

[Cerda et al. 2002] E. Cerda, K. Ravi-Chandar, and L. Mahadevan, "Wrinkling of an elastic sheet under tension", *Nature* **419** (2002), 579–580.

[DuPont 2001] DuPont, "Summary of properties for Kapton polyimide film", 2001, Available at http://www.dupont.com/kapton.

[Epstein 2003] M. Epstein, "Differential equation for the amplitude of wrinkles", *AIAA Journal* **41** (2003), 327–329.

[Jenkins 2001] C. H. Jenkins, *Membrane and inflatable structures technology for space applications*, AIAA, Reston, VA, 2001.

[Jenkins et al. 1998] C. H. Jenkins, F. Haugen, and W. H. Spicher, "Experimental measurement of wrinkling in membranes undergoing planar deformation", *Experimental Mechanics* **38** (1998), 147–152.

[Mansfield 1968] E. H. Mansfield (editor), *Tension field theory a new approach which shows its duality with inextensional theory*, 1968.

[Mansfield 1970] E. H. Mansfield, "Load transfer via a wrinkled membrane", *Proc. R. Soc. Lond. A.* **316** (1970), 269–289.

[Mansfield 1989] E. H. Mansfield, *The bending and stretching of plates*, 2nd ed., Cambridge University Press, 1989.

[Mikulas 1964] M. M. Mikulas, "Behavior of a flat stretched membrane wrinkled by the rotation of an attached hub", NASA, 1964.

[Murphey 2000] T. W. Murphey, *A nonlinear elastic constitutive model for wrinkled thin films*, Ph.D. thesis, Department of Mechanical Engineering, University of Colorado at Boulder, 2000.

[Papa and Pellegrino 2005] A. Papa and S. Pellegrino, "Mechanics of systematically creased thin-film membrane structures", pp. 18–21 in *46th AIAA/ASME/ASCE/AHS/ASC Structures, Structural Dynamics and Materials Conference*, Austin, TX, April 2005 2005. AIAA 2005-1975.

[Reissner 1938] E. Reissner, "On tension field theory", pp. 88–92 in *Proc. 5th Int. Cong. Appl. Mech.*, 1938.

[Stein and Hedgepeth 1961] M. Stein and J. M. Hedgepeth, *Analysis of partly wrinkled membranes*, NASA Langley Research Center, 1961.

[Wagner 1929] H. Wagner, "Flat sheet metal girder with very thin metal web", *Zeitschrift für Flugtechnik Motorluftschiffahrt* **20** (1929), 200–207, 227–233, 256–262, 279–284.

[Wong 2003] Y. W. Wong, *Wrinkling of thin membranes*, Ph.D. thesis, University of Cambridge, 2003.

[Wong and Pellegrino 2002] Y. W. Wong and S. Pellegrino, "Amplitude of wrinkles in thin membrane", pp. 257–270 in *New approaches to structural mechanics, shells and biological structures*, edited by H. Drew and S. Pellegrino, Kluwer, 2002.

[Wong and Pellegrino 2006a] Y. W. Wong and S. Pellegrino, "Wrinkled membranes II: analytical models", *J. Mech. Materials Struct.* **1** (2006), 27–61.

[Wong and Pellegrino 2006b] Y. W. Wong and S. Pellegrino, "Wrinkled membranes III: numerical simulations", *J. Mech. Materials Struct.* **1** (2006), 63–95.

Received 3 Mar 2005. Revised 10 Oct 2005.

Y. WESLEY WONG: wesleywong@cantab.net

SERGIO PELLEGRINO: pellegrino@eng.cam.ac.uk
Department of Engineering, University of Cambridge, Trumpington Street, Cambridge, CB2 1PZ, United Kingdom